ISSN 0015-4628, Fluid Dynamics, 2013, Vol. 48, No. 5, pp. 687–696. © Pleiades Publishing, Ltd., 2013.
Original Russian Text © Yu.A. Vinogradov, A.G. Zditovets, M.M. Strongin, 2013, published in Izvestiya Rossiiskoi Akademii Nauk, Mekhanika Zhidkosti i Gaza, 2013, Vol. 48, No. 5, pp. 134–145.

Experimental Investigation of the Temperature Stratification of an Air Flow through a Supersonic Channel with a Central Body in the Form of a Porous Permeable Tube

Yu. A. Vinogradov, A. G. Zditovets, and M. M. Strongin

Received November 12, 2012

Abstract—The results of an experimental investigation of the gasdynamic temperature separation (stratification[1]) of a supersonic air flow are presented. It is shown that in an axisymmetric supersonic channel the presence of a central body in the form of a cylindrical tube consisting of impermeable and permeable sections leads to the redistribution of the total energy of the flow. At the central body exit the mass-mean stagnation temperature of the air increases compared with its initial temperature.

Keywords: gasdynamic temperature stratification, supersonic flow, powerless techniques of energy separation, temperature recovery coefficient.

DOI: 10.1134/S0015462813050128

There is much research devoted to the temperature stratification of gas flows. An overview of these studies can be found in [1]. On the basis of the temperature stratification phenomenon the powerless techniques of energy separation of gas flows have been developed. The distinctive feature of the devices based on the powerless techniques is the absence of mechanisms powered by the gas flow, such as pistons, blades, etc. In these devices the gas does not make external work and does not take part in the heat transfer to the surrounding. Thus, a gas flow with an initial stagnation temperature T_0^* having passed through this device is divided into as minimum two flows with the stagnation temperatures $T_1^* < T_0^*$ and $T_2^* > T_0^*$, that is, the powerless energy separation of the gas flow is realized. The most widespread techniques of powerless energy separation include the vortex and resonance methods realized in the Ranque–Hilsch vortex tubes and the Hartmann–Sprenger resonance tubes. At present, there are many types of these devices which have found the application in the industry [2–6]. Their advantages are the simplicity of manufacturing, high reliability, low inertia, the absence of lubrication systems, and the possibility of operating on a wide range of the working body temperatures. On the other hand, they possess a considerable shortcoming which restricts their application in thermal engines and heating plants: this is the high total pressure loss of both cold and hot flows. In [7] a new method of the powerless energy separation of a gas flow was proposed; in this method at the device exit the total pressure is almost conserved for one of two flows. The basic diagram of a powerless energy separation device realizing this method is presented in Fig. 1.

The compressed gas (air, vapor, gas mixture, etc.) supply is taken from the plenum chamber *1* with the stagnation parameters T_0^* and P_0^* into the working section, where it is divided by partition *2* into two flows *3* and *4*. Flow *3* is not subjected to the geometric effect and remains subsonic, while flow *4* is accelerated in nozzle *5* up to a supersonic velocity. It is known [8] that the temperature of a thermally insulated plane wall in a gas flow is determined by the expression

[1]The term *stratification* is used in accordance with the terminology introduced in [1].

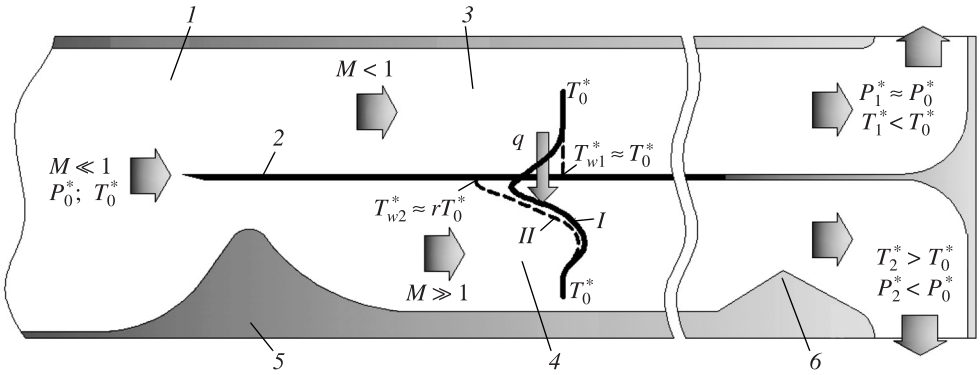

Fig. 1. Basic diagram of a device for powerless energy separation of a flow using the Leont'ev method; (*1*) plenum chamber; (*2*) separating partition; (*3*) subsonic flow; (*4*) supersonic flow; (*5*) supersonic nozzle; and (*6*) supersonic diffuser. Stagnation temperature distribution in the boundary layer in the cases of heat-conducting (*I*) and thermally-insulated (*II*) partitions.

$$T_w^* = \frac{T_0^*(1 + r0.5(k - 1)\mathrm{M}^2)}{1 + 0.5(k - 1)\mathrm{M}^2}, \tag{0.1}$$

where k is the adiabatic exponent, M is the undisturbed flow Mach number, and r is the temperature recovery coefficient. In the case of a subsonic flow ($\mathrm{M} \ll 1$) from Eq. (0.1) it follows that $T_w^* \approx T_0^*$, while in the supersonic case ($\mathrm{M} \gg 1$) it can be taken that $T_w^* \approx rT_0^*$. In Fig. 1 the broken curve presents the stagnation temperature profiles in the boundary layers of supersonic and subsonic flows (partition *2* is a flat thermally insulated plate and $r < 1$). The partition surface temperatures on the subsonic (T_{w1}^*) and supersonic (T_{w2}^*) flow sides are different. Therefore, if the partition is made heat-conducting, then the heat transfer between the two flows begins. In this case, the supersonic flow is heated and the subsonic flow is cooled. In this device $T_w^* \approx rT_0^*$ is the greatest, theoretically permissible temperature of the subsonic flow cooling. If $r > 1$, then the heat flux is directed in the opposite direction. At $r = 1$ the heat transfer between the two flows is absent and energy separation does not occur. The specific heat flux is determined by the expression

$$q = \frac{T_{w1}^* - T_{w2}^*}{1/\alpha_1 + \delta/\lambda + 1/\alpha_2} = K(1 - r)T_0^*, \tag{0.2}$$

where q is the specific heat flux in W/m^2, $K = 1/(1/\alpha_1 + \delta/\lambda + 1/\alpha_2)$ is the heat transfer coefficient in W/(m^2 K), α_1 and α_2 are the heat transfer coefficients on the supersonic and subsonic flow sides in W/(m^2 K), δ is the thickness of the flow-separating partition in m, and λ is the thermal conductivity of the material in W/(m K).

We will consider in more detail the methods of influencing the temperature recovery coefficient which could be applied for enhancing the temperature stratification in the device under consideration.

As shown in [9–11], the application of a surface relief (holes, grooves, annular protrusions, notches, etc.) on a plate leads to a reduction of the surface-average temperature recovery coefficient. Depending on the surface relief the local values of r can vary within the limits from 0.82 to 0.91 and the surface-average values from 0.85 to 0.87; thus, one of the means of enhancing the temperature stratification is the application of the surface relief on the partition *2* (Fig. 1) on the supersonic flow side.

The temperature recovery coefficient can be very considerably reduced on a porous permeable surface through which gas is blown into a supersonic boundary layer. The most known experimental results are presented in Fig. 2 [12]. In this figure the temperature recovery coefficient is plotted against the permeability parameter $b_M = j/\mathrm{St}_M$, where $j = (\rho v)_w/(\rho u)_0$ is the relative injection intensity, $(\rho v)_w$ and $(\rho u)_0$ are the mass velocities of the injected gas and the main flow in kg/(m^2 s), and St_M is the Stanton number at the same incident flow parameters (Mach and Reynolds numbers) and $j = 0$. In [18] on the basis of a numerical investigation the dependence $r = r_0(1 - 0.04b_M)$ was proposed for determining the recovery coefficient on

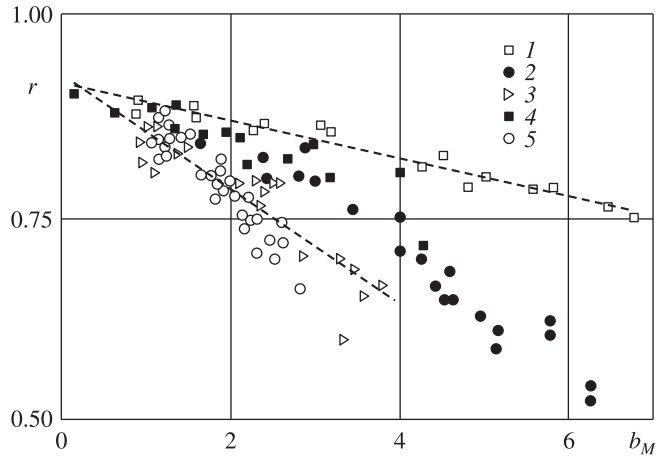

Fig. 2. Experimental dependence of the temperature recovery coefficient r on the injection parameter $b_M = j/\mathrm{St}_M$; (*1*) [13], M = 3.2; (*2*) [14], M = 2.5; (*3*) [15], M = 2.3; (*4*) [16], M = 3; and (*5*) [17], M = 2.7; broken lines approximate the experimental data.

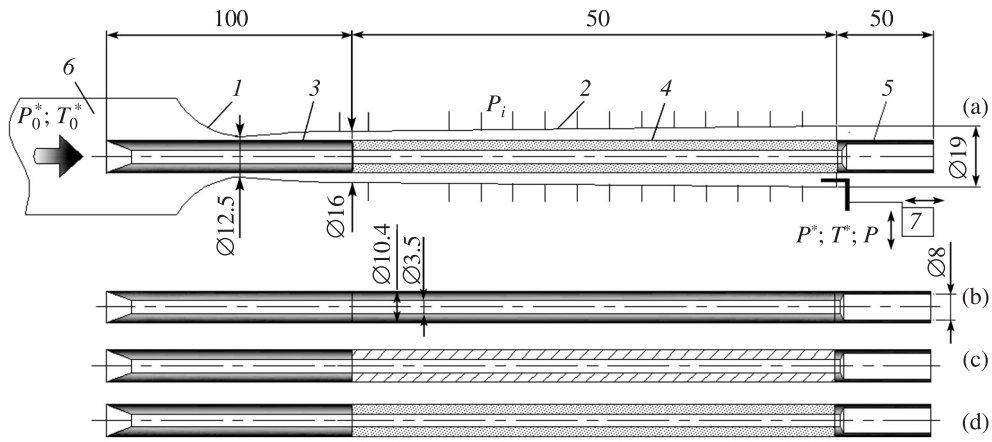

Fig. 3. Diagram of the working part of the experimental setup (a); (*1*) supersonic contoured nozzle; (*2*) conical tube (ebonite); (*3*) impermeable tube (ebonite); (*4*) working section of the central body; (*5*) exit diffuser; (*6*) plenum chamber; and (*7*) coordinate device; (b–d) are the model central bodies.

a porous permeable surface with gas injection; here, r_0 is the recovery coefficient on an impermeable flat plate. Clearly, gas injection ($b_M \neq 0$) into a supersonic boundary layer can lead to a considerable reduction in the temperature recovery coefficient r on the permeable plate as compared with the impermeable plate.

The gas injection effect on the amount of the heat transferred from the subsonic to the supersonic flow was theoretically considered in [1, 7, 19, 20]. The case of an impermeable wall was theoretically considered in [1, 7, 19–24].

The purpose of this study is an experimental investigation of the temperature stratification process in a device realizing the Leont'ev method, where a porous permeable surface is used a separating wall.

1. MODELS AND EXPERIMENTAL CONDITIONS

The experimental investigation was carried out in the hypersonic aerodynamics laboratory of the Institute of Mechanics of the Moscow State University. The working section of the rig is schematically presented in Fig. 3a.

An axisymmetric contoured supersonic nozzle *1* smoothly goes over into the conical tube *2* thus forming a supersonic channel. In the study three model central bodies differing in the working section material

were used (Fig. 3b–3d); (b) is model *1* with the working section made of heat insulator (ebonite, $\lambda = 0.16$ W/(m K) [25]); (c) is model *2* or a heat-conducting working section (copper tube, $\lambda = 384$ W/(m K) [25]); and (d) is model *3* or a permeable tube (sintered electrocorundum, $\lambda = 40$ W/(m K) [26], open porosity of 37 to 38%, the pore diameter of 60 to 65 μm, and the density of 2210 kg/m^3). During the rig operation the air from the plenum chamber *6* arrives to two channels; the first is the inner channel of the central body and the second is the annular channel formed by the inside surfaces of the supersonic nozzle and the conical tube and the outside surface of the central body. In the outer channel the air is accelerated to a supersonic velocity in the supersonic nozzle. At the nozzle exit the nominal Mach number M = 2.66. In the same section of the inner channel the flow remains subsonic. Then it is the material of the working section of the model central body that determines the nature of the interaction between the inner and outer flows. Thereupon the inner flow is decelerated in diffuser *5*, while the outer flow flows out directly into the atmosphere.

The investigation included the following measurements. On the lateral surface of the conical tube *2* (Fig. 3a) there were static pressure heads located at 26 points (13 points on each side); one more head was near the supersonic nozzle exit. In the plenum chamber there were three stagnation pressure (P_0^*) heads and four stagnation temperature (T_0^*) probes. The profiles of the total P^* and static P_i pressures and the stagnation temperature T^* of the outer and inner flows were measured using special probes [27] fastened on the coordinate device *7* (Fig. 3a). A maximum depth of probe immersion amounted to 40 mm from the exit section of the conical tube. The outside diameter of the pressure probes was 1.2 mm and that of the stagnation temperature probe was 1.6 mm. The pressure was measured with the pressure transducers. The temperature measurements were carried out using chromel-nickel thermocouples. In measuring the stagnation temperature in the plenum chamber the absolute random error was $\pm 0.3°$C and in measuring the stagnation temperature profile by means of the probe it was $\pm 0.6°$C.

The investigation included three stages. In the first stage the central body was the heat insulator (Fig. 3b). The data obtained in this case corresponded to the regime in which there is no interaction between the flows. They provided the basis for estimating the energy separation amount in the subsequent stages. In the second stage model *2* was used (Fig. 3c); in this form the setup operated in accordance with the diagram presented in Fig. 1. In the third stage the model central body included a permeable section (Fig. 3d). In all the stages the stagnation parameters in the plenum chamber (pressure and temperature) were maintained the same. The measurements were carried out only after a steady regime has been attained.

2. RESULTS

In Fig. 4 the stagnation temperature and Mach number profiles in the inner and outer flows are plotted for the three model central bodies. In the outer flow the measurements were performed at a distance of 7 mm from the exit section of the conical tube and in the inner flow they were carried out at a distance of 10 mm from the exit section of the central body diffuser. The Mach number profiles were calculated from the values of the total and static pressures measured by the corresponding probes at the corresponding points.

In the first stage model *1* (heat insulator) was used as the central body. In this case, there was no interaction between the flows. Therefore, the mean-mass stagnation temperatures in the inner and outer channels were the same and equal to the stagnation temperature in the plenum chamber. Before turning to the temperature profiles presented in Fig. 4b we will note the important feature concerning the stagnation temperature measurement by means of probes in a high-velocity flow. The temperature measured by the thermocouple of the probe is different from the actual stagnation temperature at this point being somewhat lower [27]. For any particular probe design on a wide temperature range this difference depends only on the velocity of the flow past the temperature probe. In particular, the temperature presented in Fig. 4b is that measured by the probe rather than the actual stagnation temperature of the flow. However, in view of the fact that the Mach number distributions along the inner channel are similar in shape for all the three models (Fig. 4c), the measurements were carried out using the same probe, and the stagnation temperature range is small, it may be assumed that at each point of a cross-section the difference in the stagnation temperature,

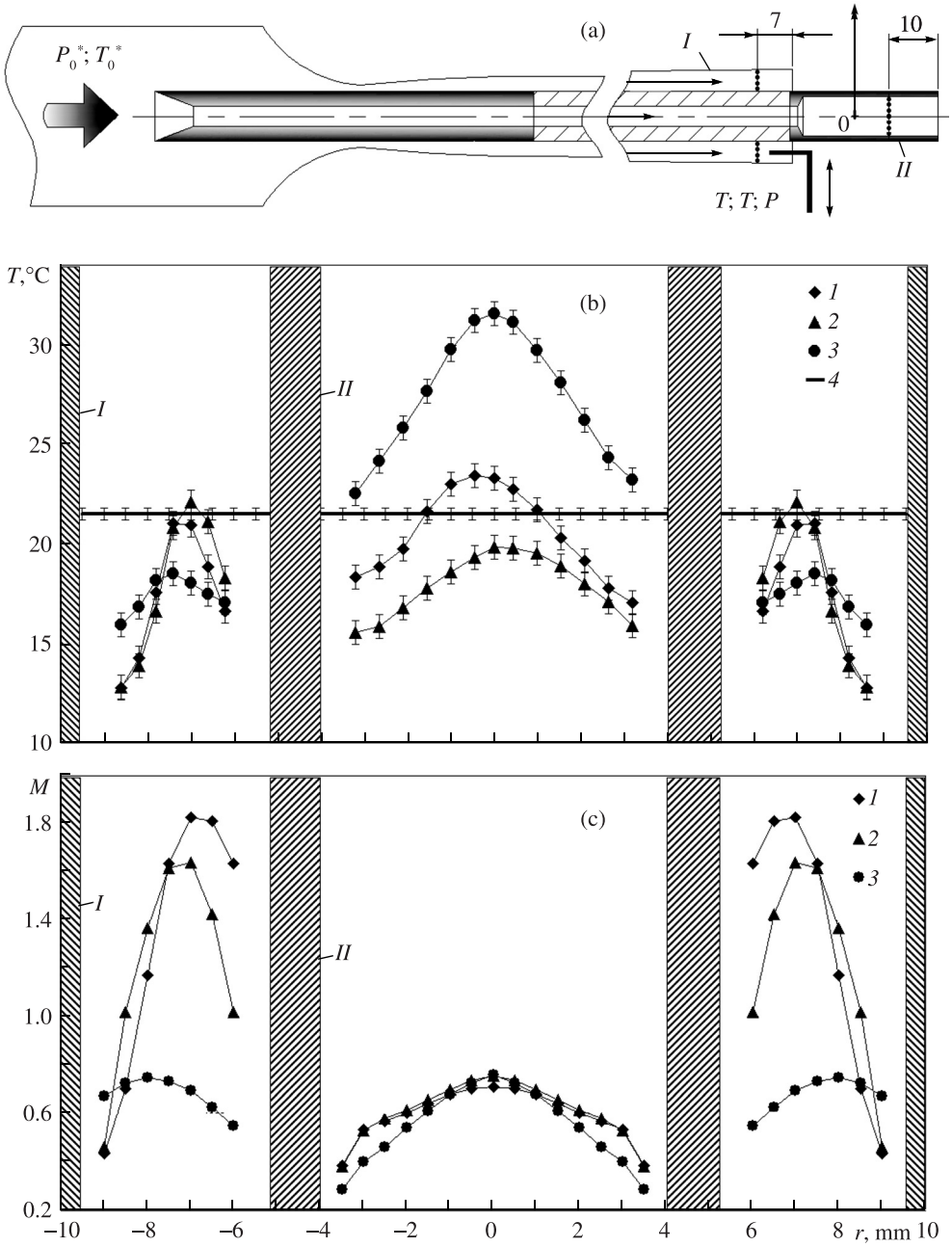

Fig. 4. Setup (a) and flow temperature (b) and Mach number (c) profiles measured at distances of 7 mm from the exit section of the outer channel (*I*) and 10 mm from the exit section of the exit diffuser (*II*); (*1–3*) are models (*1–3*) and (*4*) is the stagnation temperature in the plenum chamber, $21.5 \pm 0.3°$C.

when one model was replaced by another, was fixed with a sufficient degree of accuracy. Since in the outer channel at the point of measurement of the stagnation temperature (Fig. 4a) the Mach number profiles (Fig. 4c) are considerably different for different models, in this case the conclusions on the basis of the measured data should be made with caution. In what follows, we will discuss only the temperature profiles measured at the central body exit.

The stagnation temperature in the plenum chamber was $21.5 \pm 0.3°$C, while the mean-mass temperature measured by the probe at the model *1* exit was $18.6 \pm 0.6°$C. This temperature is lower than the stagnation temperature in the plenum chamber in view of the reasons presented above. It was used as the reference temperature in determining the energy separation in the case of models *2* and *3*. In the case of model *2* with a heat-conducting working section heat transfer between the flows arose. As can be seen in Fig. 4b, in this case the temperature profile lies lower; therefore, the heat is removed from the flow. The mean-mass temperature was $17.2 \pm 0.6°$C. So small difference in the mean-mass temperatures is attributable to the fact that for the given thermal conductivity value $K = 0.2$ the area of the working surface of model *2*, through which the heat transfer was realized, was insufficient for realizing the available temperature head. Thus, both the heat transfer area and the thermal conductivity must be increased in order to enhance the energy separation effect (all other things being the same).

An interesting result was obtained in the case of model *3*. The mean-mass temperature at the central body exit turned out to be $25.8 \pm 0.6°$C which is about 7°C higher than in the absence of the interaction between the flows (model *1*). It was necessary to understand the reason for heating the inner flow. As shown in Fig. 2, gas injection into the supersonic flow reduces the temperature recovery coefficient and, therefore, a more intense heat transfer between the flows and a more considerable reduction in the temperature at the central body exit than in the case of model *2* might be anticipated [1, 7, 19].

With this in mind, we measured the total and static pressure profiles in the inner and outer channels at distances of 20 and 30 mm from the exit section of the outer channel (Fig. 5a). In this case, the central body (model *3*) had no central diffuser. The further immersion of the probe was limited by its design features. It turned out that on the measured depths the flow within the porous permeable tube is supersonic, while in the annular channel it is subsonic (Fig. 5b).

The result obtained can be explained as follows: the air flow which entered the inner cylindrical channel of the impermeable section of the central body *3* (Fig. 3a) is accelerated up to a supersonic velocity at the beginning of the porous permeable section. This can happen only at the expense of the work of friction forces, since in this stage the action on the flow of other types (geometrical, thermal, flow-rate, and mechanical) was absent. The one-dimensional flow with friction in the cylindrical tube was calculated using the method described in [28] under the conditions realized in this study (the cylindrical channel length-to-diameter ratio $l/d \approx 30$). It was assumed that the flow is stabilized (the initial region was not considered), while the friction coefficient ζ was determined from the equation $1/\zeta^{0.5} = 2\log(\mathrm{Re}_d\zeta^{0.5}) - 0.8$, where Re_d is the Reynolds number based on the tube diameter [8].

The calculations showed that a minimum pressure ratio necessary for realizing a sonic regime in the exit section of the impermeable tube $(P_0^*/P_1)_{\min} = 2.159$, where P_1 is the static pressure of the medium into which the gas flows out. The working ratio realized in the experiment $P_0^*/P_l = 7.5$ (if we assume that the gas flows out in the atmosphere). Therefore, it can be concluded that in the inner channel of model *3*, in the section, where the impermeable tube was connected with the porous permeable tube (Fig. 3), the air flows at the sonic velocity.

The other part of the flow (outer flow), which has passed through the supersonic nozzle, moves in the same section with a supersonic velocity. Since the stagnation parameters of the two flows are the same, the static pressure of the supersonic flow is smaller than that of the sonic (inner) flow; therefore, gas is injected from the inner into the outer channel.

The flow in the inner channel of the porous permeable tube experiences the actions of three types, namely, the so-called flow-rate action and the thermal and friction actions. Depending on the relationship between these actions, the flow moving at the sonic velocity can both be accelerated up to a supersonic velocity and

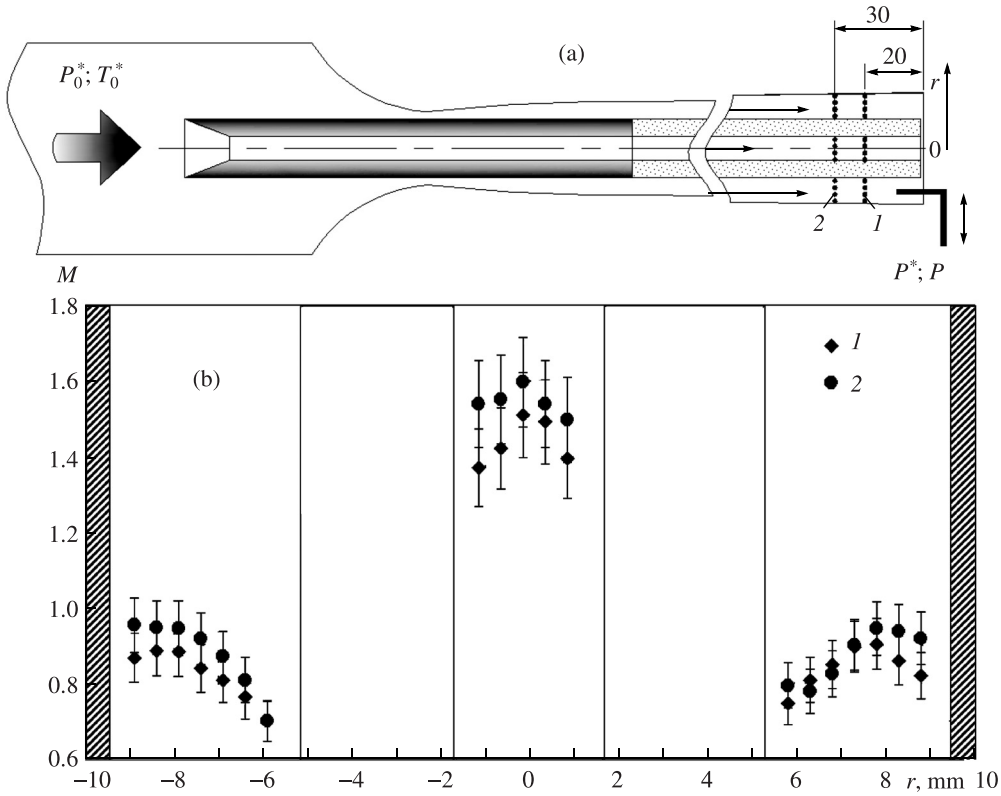

Fig. 5. Setup (a) and Mach number distribution in the cross-sections of the inner and outer channels (b); depth of 20 and 30 mm (*1*, *2*); the central body is model (*3*) without the exit diffuser.

be decelerated down to a subsonic velocity. The measurements made in this study showed that at the channel exit the flow was supersonic and its temperature was greater than in the plenum chamber (Figs. 4b and 5b).

It is known that gas suction from a supersonic flow leads to its acceleration, while heat supply and friction work decelerate a supersonic flow [29]. Therefore, under the conditions realized in the experiment the flow-rate action (suction) was predominant over the other actions on the flow and made it possible to accelerate it from the sonic to a supersonic velocity. The experimental data on the sonic flow acceleration up to supersonic velocities using suction through a permeable wall can be found in [30].

We will now consider the flow in the annular channel. At the supersonic nozzle exit, at the point with the coordinate $x = -4$ mm (point of static pressure receiver in Fig. 6) the flow was supersonic, $\mathrm{M} = 2.60 \pm 0.05$. From the beginning of the porous section ($x = 0$), additionally to the actions of the three types described above, the flow experiences the geometrical action due to the channel conicity. The probe measurements showed (Fig. 5) that at the depth of 30 mm ($x = 120$ mm) the flow is subsonic. To understand the flow rate (injection) effect on the supersonic flow in the annular channel we will consider the flow in this channel in the absence of the flow-rate action, with the identical parameters in the plenum chamber (flows with models *1* and *2*).

In Fig. 6 the static pressure distribution along the annular channel length is presented for the models of all the three types. In the case of models *1* and *2* the static pressure profile is smooth and the pressure slowly decreases to $x = 120$ mm. Therefore, in the region from $x = -4$ to $x = 120$ mm the air flow remains supersonic and is accelerated somewhat, that is, the effect of the channel area-of-passage expansion due to conicity is predominant over the effects of the friction work and the area-of-passage contraction at the expense of the growing boundary layer. Then, starting from $x = 120$ mm the flow is decelerated in a "pseudoshock" (region of supersonic-to-subsonic flow transition). This pattern, typical of supersonic flow deceleration in channels, is described in detail in [31].

In the presence of the flow-rate (injection) effect (Fig. 6, model *3*) the static pressure profile considerably

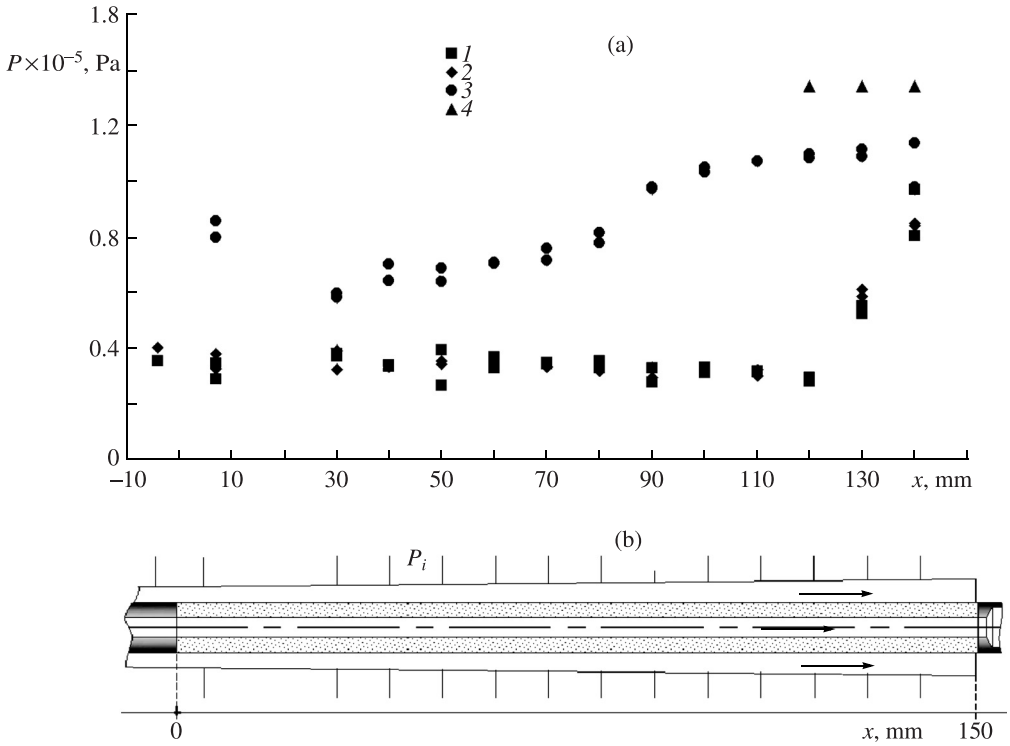

Fig. 6. Static pressure distribution (a) along the length of the outer annular channel and within the porous permeable tube (model *3*); the stagnation pressure in the plenum chamber $P_0^* = 7.4 \times 10^{-5}$ Pa; (*1–3*) are models (*1–3*, *4*) is the inner channel of model (*3*); diagram of the location of the static pressure heads (b).

changes. At the point with the coordinate $x = 7$ mm there is a static pressure splash due to the beginning of injection into the supersonic flow and then a continuous static-pressure growth can be observable. The nature of the pressure distribution makes it possible to conclude that the supersonic flow is considerably decelerated and goes over into a subsonic flow through a "pseudoshock" on the interval from $x = 60$ to 100 mm. The probe measurements showed that at the point with the coordinate $x = 120$ mm the flow is subsonic. Thus, the mass transfer through the porous permeable region leads to flow acceleration in the inner channel up to supersonic velocities and to considerable flow deceleration in the outer annular channel. It should be noted that in the inner channel the static pressure in the probe measurement region $x = 120$ to 140 mm remains higher than the static pressure of the flow in the annular channel (Fig. 6). Therefore, it may be asserted that the mass transfer direction does not change when the flow in the annular channel becomes sonic.

We will finally turn to the discussion of the data on the energy separation (Fig. 4), that is, the mode of the flow heating in the inner channel of model *3*. We will base on the results obtained using numerical simulation of the turbulent boundary layer on a permeable surface [20]. We will consider the integral energy relation derived on the basis of the energy equation for the stagnation enthalpy $h^* = h + 0.5u^2$, when the gas flows along a cylindrical channel in the presence of mass transfer

$$\frac{d}{dx}\int_0^{r_0} \rho u\left(h^* - h_0^*\right)\frac{r}{r_0}\,dr = \rho v(h_0^* - h_w^*) + \frac{\lambda}{C_p}\left(\frac{dh^*}{dr}\right)_w = q_j - q_w, \tag{2.1}$$

where x is the longitudinal coordinate, r and r_0 are the current radius and the tube radius, h_0^* is the stagnation enthalpy in the undisturbed flow (at the tube entry), h_w^* is the gas stagnation enthalpy at $r = r_0$, q_j is the convective enthalpy flux, $q_w = -\lambda/C_p(dh^*/dr)_w$ is the diffusive heat flux to the wall, and λ and C_p are thermal conductivity and specific heat of the gas. The derivation of an analogous relation in the case of a plane flow can be found in [32].

From Eq. (2.1) it follows that a variation in the stagnation enthalpy of a gas flow that takes part in heat and mass transfer, is possible at the expense of the diffusive and convective mechanisms of the stagnation enthalpy transfer through the wall separating the interacting gas flows. The relations between these flows for different relative velocities of the interacting gas flows are considered in detail in [20]. The internal flow heating can be explained on the basis of the assumption that at a certain distance from the beginning of the porous section this flow acquires a velocity higher than that of the external flow, which is experimentally confirmed at $x = 120$ mm (Fig. 6). In this case, $h_w^* < h_0^*$ and the terms on the right side of Eq. (2.1) are summed, since the diffusive heat flux is directed from the external to the internal flow. The convective enthalpy transfer favors the removal of the "cold" gas of wall layers from the boundary layer of the internal flow, thus increasing the temperature of the remaining gas. Thus, the gas suction from the inner channel not only accelerates the flow up to supersonic velocities but also favors the enhancement of the energy separation of the flows due to the addition of the diffusive and convective heat transfer mechanisms.

To provide a deeper understanding of the processes occurring during the acceleration of the gas flow moving in a channel with permeable walls in the presence of the thermal and flow-rate actions up to supersonic velocities an experimental investigation must be performed with large-scale models which would make it possible to obtain the local flow parameters with a high accuracy and reliability.

Summary. The experimental data confirming the possibility of powerless energy separation of a supersonic air flow are obtained. It is shown that the presence of a central body with a permeable section in a channel leads to heat and mass flux redistribution. As a result, the stagnation temperature of the gas issuing of the central body is greater than that of the gas flowing out of the supersonic channel.

The study was carried out with the support of a grant of the President of the Russian Federation MK-56.2011.8 and the Russian Foundation for Basic Research (projects Nos. 11-08-00152 and 12-08-33009).

REFERENCES

1. A.I. Leont'ev, "Gas-Dynamic Methods of Temperature Stratification (a Review)," Fluid Dynamics **37** (4), 512 (2002).
2. A.V. Martynov and V.M. Brodyanskii, *What Is a Vortex Tube* [in Russian], Svyaz, Moscow (1976).
3. Sh.A. Piralishvili, V.M. Polyaev, and M.N. Sergeev, "Vortex Effect: Experiment, Theory, and Engineering Solutions," [in Russian], Energomash, Moscow (2000).
4. H. Sprenger, "Über thermische Effekte in Resonanzrohren," Mitt. Inst. Aerodynamik No. 21, 18 (1954).
5. Yu.B. Eliseev and A.Ya. Cherkez, "On the Heating Effect in Gas Flow over Deep Cavities," Fluid Dynamics **6** (3), 368 (1971).
6. A.M. Arkharov, I.V. Marfenina, and E.I. Mikulin, *Cryogenic Systems. Vol. 1*, [in Russian], Mashinostroenie, Moscow (1996).
7. A.I. Leont'ev, "Temperature Stratification of a Supersonic Gas Flow," Dokl. Ross. Akad. Nauk **354**, 475 (1997).
8. H. Schlichting, *Boundary Layer Theory*, McGraw-Hill, New York (1968).
9. P. Brinich, "Recovery Temperatures and Heat Transfer near Two-Dimensional Roughness Elements at Mach 3.1," NACA Techn. Rep. No. 4213 (1958).
10. A.I. Leontiev, Yu.A. Vinogradov, S.M. Bednov, A.N. Golikov, I.K. Ermolaev, E.V. Dilevskaya, and M.M. Strongin, "Effect of Vortex Flows at Surface with Hollow-Type Relief on Heat Transfer Coefficients and Equilibrium Temperature in Supersonic Flow," Exp. Thermal Fluid Sci. **26**, 487 (2002).
11. A.G. Zditovets and A.A. Titov, "Effect of the Surface Shape of a Thermally Insulated Rod in a Supersonic Flow on the Temperature Recovery Coefficient," Izv. Ross. Akad. Nauk. Energetika No. 2, 111 (2007).
12. S.S. Kutateladze and A.I. Leont'ev, *Heat and Mass Transfer and Friction in Turbulent Boundary Layers* [in Russian], Energoatomizdat, Moscow (1985).
13. E.B. Bartle and B.M. Leadon, "Experimental Evaluation of Heat Transfer with Transpiration Cooling in a Turbulent Boundary Layer at M = 3.2," J. Aerospace Sci. **27**, 78 (1960).
14. Yu.V. Baryshev, Yu.A. Vinogradov, A.I. Leont'ev, and V.I. Rozhdestvenskii, "Recovery Factors for a Permeable Surface and a Gas Surface Film in a Supersonic Turbulent Boundary Layer," Fluid Dynamics **7** (2), 303 (1972).

15. N.I. Yarygina, *Heat Transfer and Friction in a Compressible Turbulent Boundary Layer on a Permeable Surface*, Candidate's Dissertation in Technical Sciences, Novosibirsk (1971).
16. B.M. Leadon and C.J. Scott, "Transpiration Cooling Experiments in a Turbulent Boundary Layer at M = 3," J. Aeronaut. Sci. **23**, 798 (1956).
17. M.W. Rubesin, C.C. Pappas, and A.F. Okuno, "The Effect of Fluid Injection on the Compressible Turbulent Boundary Layer—Preliminary Tests on Transpiration Cooling of a Plate at M = 2.7 with Air as the Injected Gas," NACA RM A55119 (1955).
18. A.I. Leont'ev, V.G. Lushchik, and A.E. Yakubenko, "Temperature of a Thermally-Insulated Permeable Wall in a Compressible Flow," Fluid Dynamics **43** (5), 789 (2008).
19. S.A. Burtsev and A.I. Leont'ev, "Temperature Stratification in a Supersonic Gas Flow," Izv. Ross. Akad. Nauk. Energetika No. 5, 101 (2000).
20. A.I. Leont'ev, V.G. Lushchik, and A.E. Yakubenko, "Injection/Suction Effect on Energy Separation in Compressible Flows," Fluid Dynamics **46** (6), 935 (2011).
21. S.A. Burtsev, "Investigation of Temperature Stratification in a Gas," Vestn. Mosk. Gos. Tekhn. Un-ta. Ser. Mashinostroenie No. 2, 65 (1998).
22. S.A. Burtsev, "Optimization of the Supersonic Channel Geometry in a Energy Separation Device," Vestn. Mosk. Gos. Tekhn. Un-ta. Ser. Mashinostroenie No. 2, 48 (1999).
23. I.I. Vigdorovich and A.I. Leont'ev, "Theory of the Energy Separation of a Compressible Gas Flow," Fluid Dynamics **45** (3), 434 (2010).
24. E.P. Volchkov and M.S. Makarov, "Gasdynamic Temperature Stratification in a Supersonic Flow," Izv. Ross. Akad. Nauk. Energetika No. 2, 19 (2006).
25. V.S. Chirkin, *Thermal Properties of Materials* [in Russian], Fizmatgiz, Moscow (1959).
26. R.E. Krzhizhanovskii and Z.Yu. Shtern, *Thermal Properties of Nonmetallic Materials (Oxides)* [in Russian], Energiya, Leningrad (1973).
27. A.N. Petunin, *Measurement of Gas Flow Parameters. Instruments for Measuring Pressure, Temperature, and Velocity*, [in Russian], Mashinostroenie, Moscow (1974).
28. G.N. Abramovich, *Applied Gas Dynamics* [in Russian], Nauka, Moscow (1974).
29. L.A. Vulis, *Thermodynamics of Gas Flows*, [in Russian], Gosenergoizdat, Moscow (1950).
30. G.L. Grozdovskii, A.A. Nikol'skii, G.P. Svishchev, and G.I. Taganov, *Supersonic Gas Flows within Perforated Boundaries*, [in Russian], Mashinostroenie, Moscow (1967).
31. O.V. Gus'kov, V.I. Kopchenov, I.I. Lipatov, V.N. Ostras', and V.P. Starukhin, *Processes of Supersonic Flow Deceleration in Channels*, [in Russian], Fizmatlit, Moscow (2008).
32. B.S. Petukhov, *Heat Transfer in a Single-Phase Medium in Motion. Laminar Boundary Layer*, [in Russian], Moscow Energy Institute, Moscow (1993).